Ion–DNA Interactions

International Edition: DOI: 10.1002/anie.201503770
German Edition: DOI: 10.1002/ange.201503770

Can A Denaturant Stabilize DNA? Pyridine Reverses DNA Denaturation in Acidic pH

*Guillem Portella, Montserrat Terrazas, Núria Villegas, Carlos González, and Modesto Orozco**

Abstract: *The stability of DNA is highly dependent on the properties of the surrounding solvent, such as ionic strength, pH, and the presence of denaturants and osmolytes. Addition of pyridine is known to unfold DNA by replacing π–π stacking interactions between bases, stabilizing conformations in which the nucleotides are solvent exposed. We show here experimental and theoretical evidences that pyridine can change its role and in fact stabilize the DNA under acidic conditions. NMR spectroscopy and MD simulations demonstrate that the reversal in the denaturing role of pyridine is specific, and is related to its character as pseudo groove binder. The present study sheds light on the nature of DNA stability and on the relationship between DNA and solvent, with clear biotechnological implications.*

The biological role of DNA is intimately related to its structure and stability in water solution. Full dehydration of DNA or the substitution of water by a solvent of lower polarity results in large changes in the structure of DNA.[1] Variations in ionic strength of the solution yield remarkable structural plasticity,[2] and changes in the nature of counterions can even reverse the canonical rules of duplex DNA stability.[3] Some osmolytes such as urea, formamide, guanidinium chloride, dimethylsulfoxide, and pyridine are known as chemical denaturants.[4] We recently used μs-long molecular dynamics (MD) simulations to demonstrate that the very strong denaturant properties of pyridine are related to its ability to capture microscopic unfolding events by stacking on open, solvent-exposed nucleobases.[5] Here we explore the denaturant properties of pyridine in the presence of another powerful denaturant parameter: the pH. In this work we evaluate whether the effect of these two denaturants is additive, cooperative, or anti-cooperative.

We first explored the denaturing properties of pyridine at neutral pH for three DNA duplexes with different GC content (Table 1). Results shown in Figure 1 (A,B) and Table S1 (in the Supporting Information, SI) demonstrate that the addition of pyridine (Pyr) reduces the melting temperature of duplex DNA, even at low concentration (200 and 400 mM Pyr). At physiological ionic concentration (150 mM NaCl) the A·T pairings are more susceptible to the presence of Pyr than the G·C pairings, which is in good agreement with earlier experimental findings.[4] Increasing the ionic concentration from 150 mM up to 550 mM NaCl in the presence of 400 mM Pyr practically counteracts the effect of Pyr (Table S1), showing the protective action of Na^+. Very interestingly, the addition of NaCl protects DNA from Pyr addition especially well in AT-rich sequences, thus suggesting that Na^+ is competing with Pyr for the same DNA regions.

We next studied the effect of acidic pH on the stability of duplex DNA (Table S1). The same melting experiments done in the absence of Pyr at pH 4.2 and 3.8 revealed a dramatic decrease (up to 46 degrees) in the stability of the duplexes. The effect of pH is especially large as the percentage of GC increases; suggesting that protonation of cytosines ($pK_a = 4.2$) is the main mechanism for pH-dependent unfolding of DNA. To further support this hypothesis, we repeated the melting experiments substituting cytosine by 5-methylcytosine (MetC), a modification that is known to stabilize the duplex at neutral pH.[6] Indeed, we observed a rise in melting temperature for MetC-containing DNA, which, as expected, correlates with the percentage of the CG content (Table S2). As MetC is more easily protonated ($pK_a = 4.5$) than cytosine, duplex-containing MetC are more pH-dependent than wild-type DNA. For example, the melting temperature of wild-type Seq. 3 decreases by about 46 degrees when moving from

Table 1: DNA sequences used in this work and their percentage of GC content.[a]

	Sequence (GC content)
Seq. 1	d(TATGTATATTTTGTAATTAA) (10%)
Seq. 2	d(CGTTTCCTTTGTTCTGGA) (44%)
Seq. 3	d(GTCCACGCCCGGTGCGACGG) (80%)

[a] Sequences given from 5′ to 3′, only the Watson strand is reported, the second strand is complementary in sequence.

[*] Dr. G. Portella,[+] Dr. M. Terrazas,[+] Dr. N. Villegas, Prof. Dr. M. Orozco
Institute for Research in Biomedicine (IRB Barcelona)
Joint BSC-IRB Research Program in Computational Biology
Barcelona (Spain)
E-mail: modesto.orozco@irbbarcelona.org
Prof. Dr. M. Orozco
Department of Biochemistry and Molecular Biology
University of Barcelona (Spain)
Dr. G. Portella[+]
Department of Chemistry
University of Cambridge
Cambridge CB2 1EW (UK)
Dr. N. Villegas
Barcelona Supercomputing Center
Barcelona (Spain)
Prof. Dr. C. González
Instituto de Química Física Rocasolano, CSIC
Madrid (Spain)
[+] These authors contributed equally to this work.

Supporting information for this article (including full details on the analysis of the thermal stability of DNA duplexes, NMR spectroscopy, and molecular dynamics simulations) is available on the WWW under http://dx.doi.org/10.1002/anie.201503770.

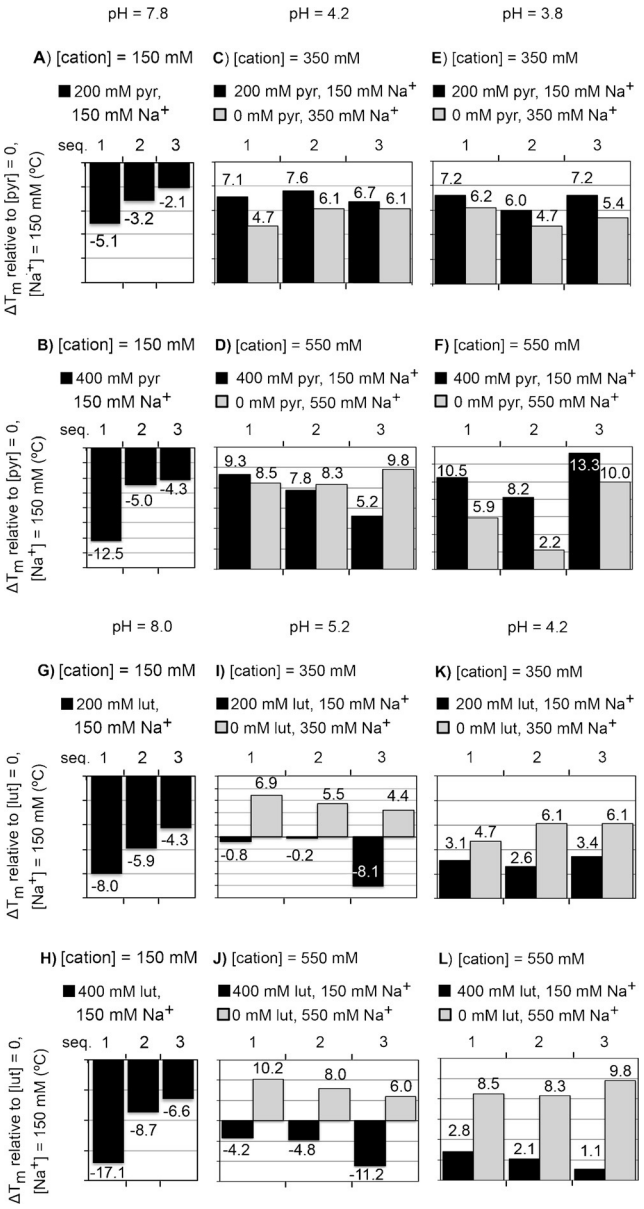

Figure 1. A–F) Effect of pyridine and Na^+ concentration on the thermal stability of DNA sequences of varying GC content at different pH values, measured as differences in melting temperature with respect to a solution containing no pyridine and 150 mM Na^+. The experiments in (A), (C), and (E) contain 200 mM of pyridine, whereas those in (B), (D), and (F) contain 400 mM of pyridine. G–L) Effect of 2,4-lutidine and Na^+ concentration on the thermal stability of DNA sequences of varying GC content at different pH values, measured as differences in melting temperature with respect to a solution containing no 2,4-lutidine and 150 mM Na^+.

pH 7.8 to 3.8; whereas the Tm difference is of about 58 degrees for the same sequence containing MetC.

Based on these results, it could be extrapolated that the addition of Pyr would decrease the stability of DNA in acidic conditions even further. Results shown in Figure 1 and Table S1 demonstrate that the opposite occurs. Setting the concentration to 200 mM of Pyr, which destabilized duplexes at neutral pH by 2–5 degrees, stabilized the same duplexes by 6–7 degrees at acidic pH (Figure 1). Increasing the concentration of Pyr to 400 mM induces a decrease of up to 12.5 degrees at neutral pH, whereas the same amount of Pyr stabilizes the same duplex by more than 10 degrees at acidic pH (Figure 1). It is therefore clear that the effect of Pyr is drastically different when added to a neutral or to an acidic solution.

The pH-dependent denaturing/renaturing effect of Pyr is likely related to its ability to be protonated at acidic pH, because at the experimental pH 90–95% of all Pyr is in the cationic state. This generates an increase in the ionic strength of the environment, which should stabilize the folded state. However, a general increase in ionic strength does not explain the magnitude of the stabilization (Figure 1), because the addition of NaCl to obtain the same cationic concentration (in the absence of Pyr) fails to completely substitute the stabilizing effect of Pyr^+. The same experiments performed with methylated DNA provide a very similar picture. Thus, at acidic pH the "denaturant" Pyr can increase the stability of the methylated version of Seq. 3 up to 17.7 degrees, which compares with 13.3 degrees found for unmodified DNA (see Tables S1 and S2). Note again that adding an equivalent concentration of NaCl does not match the stabilizing effect of Pyr^+ also for methylated DNA.

We next confirmed that the canonical double helical structure of duplex DNA is indeed preserved both at neutral and low pH in the presence of pyridine. To this end, we collected NMR spectra of AT- and GC-rich duplexes (Seq. 1 and 3) at pH values of 4.2 and 7.8 in the presence of 400 mM deuterated pyridine (see SI for details). At both pH conditions, the imino signals of the NMR spectra exhibit chemical shifts characteristic of AT and CG base pairs (Figures 2A and B, and S2). In addition, NOESY spectra (Figure 2C) show the expected cross-peak pattern for a canonical Watson–Crick duplex (i.e., AH2–TH3 contacts and medium or weak H1′–H8 cross-peaks). Although the size of these oligonucleotides is too large for a complete sequential assignment of the NMR spectra, the experimental information allows us to rule out the formation of structures different from a canonical Watson–Crick duplex in the presence of pyridine. In summary, results discussed above correspond to duplex B-DNA→single strand unfolding processes.

The results in Figure 1 and Tables S1 and S2 strongly suggest that Pyr exhibits a rather specific stabilizing effect on

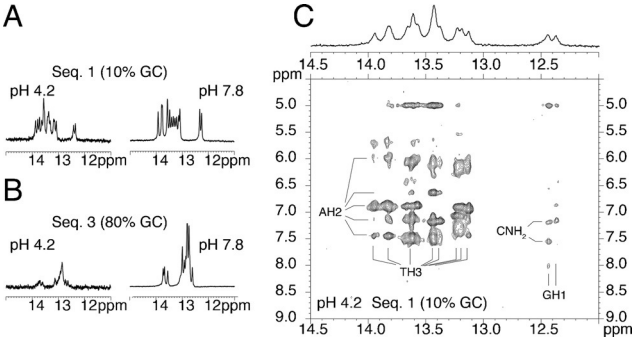

Figure 2. A,B) ^{1}H NMR spectra of the imino region of duplexes 1 and 3 acquired at pH values of 4.2 and 7.8 and in the presence of 400 mM deuterated pyridine. C) NOESY spectrum (100 ms mixing time) of duplex 1 acquired pH 4.2 and in the presence of 400 mM deuterated pyridine ($T = 5$ °C).

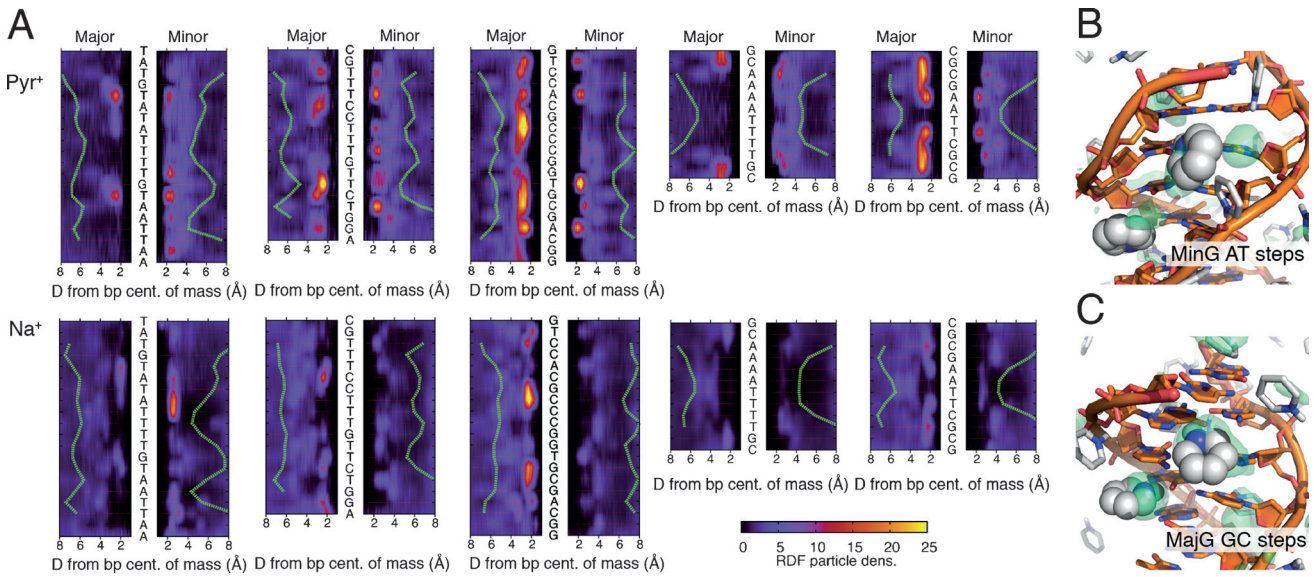

Figure 3. A) Comparison of protonated pyridine and sodium-binding positions along the major and minor grooves five different DNA sequences: the three sequences experimentally studied, the Drew–Dickerson dodecamer and GCA_4T_4GC. The sequences are specified in a top-to-bottom, 5′-to-3′, orientation for the Watson strand. The heat maps display the radial distribution function (RDF) of particle density with respect to the radial position in the major and minor grooves (plotted against the horizontal axis, reversed for the major groove) and the position along the duplex sequence (vertical axis). The reference of the RDF for both grooves is placed close to the center of the mass of the base pair. The density of solute was quantified as a function of the distance to the reference within a spherical section of 1 nm cutoff, using an angular cutoff of 2.35 rad. The green line overlaid on the maps displays the groove width (we subtracted 0.6 nm for the major groove curve). B,C) Protonated pyridine in the typical binding locations along B) minor groove (MinG) of AT steps, and along C) the major groove (MajG) of GC steps. The nonpolar pyridine hydrogen atoms and all the DNA hydrogen atoms are omitted for clarity. The green transparent volumes contain regions of pyridine nitrogen density three times larger than the corresponding bulk density (2 M pyridine).

DNA at acidic pH. To verify the specificity of the Pyr^+ stabilizing effect we repeated the melting experiments using 2,4-dimethylpyridine (2,4-Lutidine: Lut). This aromatic molecule is bulkier than Pyr, and has a pK_a of 6.63, which implies that at it should be neutral at pH 8.0 and fully protonated at pH $\leq$ 5.2. Results in Figure 2 and Table S3 demonstrate that neutral Lut is a strong denaturant (even better than Pyr). However, protonated Lut does not offer the same DNA-stabilizing effect as protonated Pyr does, and in fact the stabilization found for Lut^+ at acidic pH is smaller than that obtained by adding an equivalent quantity of NaCl (Figure 2). This confirms that the strong stabilizing effect of Pyr at acidic pH is related to short-ranged, specific duplex–Pyr^+ contacts, which are less likely to occur for the bulkier Lut molecule.

To gain detailed information on the nature of Pyr^+–DNA interactions we performed molecular dynamics (MD) simulations of duplex DNA in 2 M pyridine at low pH (all Pyrs were considered protonated), as well as control simulations in 2 M NaCl (see SI for details). We performed ten independent simulations, each 1.5 μs long for the sequences 5′-GCAAAATTTTGC-3′ (A_4T_4) and 5′-CGCGAATTCGCG-3′ (DDD), which could potentially lead to unfolding on the μs time scale.[5] To check for the generality of the conclusions derived from these calculations, additional 0.5 μs simulations were performed in 2 M NaCl, 2 M Lut^+, and Pyr^+ for Seq. 1 to 3 (Table 1), as well as for A_4T_4 and DDD. We did not observe unfolding events in any of the simulations performed (Figure S3), which is consistent with our NMR spectra, whereas previous trajectories on the same time scale and with the same force field reported several unfolding events when simulated in neutral Pyr.[5]

We traced the locations of cations (Pyr^+, Na^+, and Lut^+) in our MD simulations to explore the existence of cations placed at stable positions along the DNA, which might stabilize the entire duplex.[3,7] Analysis of cation distribution functions (Figures 3 and S4) show that protonated pyridine and sodium cation interact in a non-sequence-specific way with the phosphate groups along the DNA backbone, as can be observed by the slight increase in density at distances of about 7 Å from the base-pair center of mass in Figure 3. Furthermore, we detected regions of high Pyr^+ density along the minor (A·T) and major (G·C) grooves of DNA. When placed in the minor groove (Figure 3B) the Pyr^+ ring is positioned parallel to the groove with the acidic proton interacting directly with T(O2) and A(N3). When placed in the major groove the Pyr^+ plane is mainly oriented perpendicular to the groove with the acidic proton placed in the electronegative patch created by the N7 nitrogen and O6 oxygen of guanine (Figure 3C). Overall, the highest concentration of Pyr^+ is found in A_nT_n ($n \geq 2$) tracts in which the minor groove width is widest, for example, around the extremes of A_4T_4 sequence (5-ApA and the 3′-TpT), mimicking the situation found for choline and tetramethyl ammonium (TMA) and in agreement with previously described binding modes for a large number of cations.[7a,8] Binding specificity of sodium cations is qualitatively similar to that of Pyr^+, but the binding free energy is significantly smaller (≈ -1.4 kcal mol^{-1} for $Na+$, ≈ -2.4 kcal mol^{-1} for Pyr^+; see SI). Ion uptake experiments (SI and Table S4) show that the number of pyridine cations that condense with Seq. 3 approximately double the number of sodium cations, in good agreement with the computed binding free energy and cation densities in Figure 3. Lut^+ is

bulkier than Pyr^+ and therefore does not penetrate the DNA grooves as efficiently: few Lut^+ are bound to the major groove, and although present in the minor groove they are always placed at more distant locations from the bottom of the groove (Figure S4), which justifies their smaller stabilizing effect.

Thermodynamic analysis of the melting of duplex Seq. 3 in Pyr^+ and NaCl solutions confirmed the differential stabilization of DNA in these two solutions (Table S5), which seems to be due to enthalpic origin related to the strong interactions of well-positioned Pyr^+ in the minor grooves. As expected due to its size, Pyr^+ distorts the minor groove hydration pattern found in NaCl solutions. Thus, our simulations reveal that solvent sites in the presence of Na^+ are organized in a pattern reminiscent of a fused hexagonal motif[9] (Figure S5 A,D), and that Pyr^+ somewhat disrupts such a pattern of hydration in the minor groove (Figure S5 B,E and differential plots S5 C,F).

Our study reveals that one of the most powerful denaturants of DNA can become structure-protective when combined with another strong denaturant: acidic pH. This effect appears to be specific, as neither Na^+, nor the closely related DNA denaturant 2,4-lutidine exhibit the same behavior. Our MD simulations suggest that the denaturant properties of Pyr can be explained considering its ability to stack nucleobases,[5] whereas the protective properties of Pyr^+ are related to sequence-specific interactions of protonated pyridine molecules along the grooves of DNA. Overall, our results highlight the tunable nature of pyridine as denaturant and open new ways to alter the thermal stability of nucleic acids. The switchable behavior of the Pyr^+/Pyr pair might find applications in the field of nanobiotechnology. For example, it has been shown that a mixture of glycerol and choline chloride allows for a more efficient folding of DNA nanostructures such as DNA origamis.[10] The similar mode of interaction between choline and Pyr^+ cations with DNA suggests an avenue for the design of new DNA agents for nanobiotechnological applications, such as nanodevices with applications in photonics, litography, and electronics. Also, the tunable denaturing/renaturing effect of Pyr could aid the development of programmable fluorophore-quencher DNA-based nanoswitches such as pH nanosensors with the ability to respond to pH changes of their localized environment.[11] The structural origin of Pyr^+ stabilization could be also exploited in experiments in which DNA should be kept stable while other macromolecules are unfolded. Finally, our results could be exploited to design new cationic pyridine derivatives for the delivery of genes which should act on acidic media.[12] These potential applications of Pyr will be explored in future works.

Acknowledgements

This work was supported by the Spanish Ministry of Science (BIO2012-32868) and the European Research Council (ERC). M.O. is an ICREA Fellow. M.T. and G.P. are Miguel Servet and Sara Borrell fellows. We thank Prof. Dr. J. L. Mascareñas, Prof. Dr. R. Eritja, and Dr. E. Vázquez for their valuable comments.

Keywords: denaturant · ion–DNA interactions · molecular dynamics · NMR spectroscopy · nucleic acid thermodynamics

How to cite: *Angew. Chem. Int. Ed.* **2015**, *54*, 10488–10491
Angew. Chem. **2015**, *127*, 10634–10637

[1] a) M. K. Rueda, S. G. Kalko, F. J. Luque, M. Orozco, *J. Am. Chem. Soc.* **2003**, *125*, 8007–8014; b) S. Cui, J. Yu, F. Kühner, K. Schulten, H. E. Gaub, *J. Am. Chem. Soc.* **2007**, *129*, 14710–14716; c) A. Noy, A. Perez, C. A. Laughton, M. Orozco, *Nucleic Acids Res.* **2007**, *35*, 3330–3338.
[2] a) W. Saenger, *Principles of Nucleic Acid Structure*, Springer, New York, **1984**; b) G. S. Manning, *Biophys. Chem.* **2002**, *101–102*, 461–473.
[3] H. Tateishi-Karimata, N. Sugimoto, *Angew. Chem. Int. Ed.* **2012**, *51*, 1416–1419; *Angew. Chem.* **2012**, *124*, 1445–1448.
[4] L. Levine, J. A. Gordon, W. P. Jencks, *Biochemistry* **1963**, *2*, 168–175.
[5] A. Perez, M. Orozco, *Angew. Chem. Int. Ed.* **2010**, *49*, 4805–4808; *Angew. Chem.* **2010**, *122*, 4915–4918.
[6] a) A. Lefebvre, O. Mauffret, S. el Antri, M. Monnot, E. Lescot, S. Fermandjian, *Eur. J. Biochem./FEBS* **1995**, *229*, 445–454; b) T. K. Wojdacz, A. Dobrovic, L. L. Hansen, *Nat. Protoc.* **2008**, *3*, 1903–1908.
[7] a) G. Portella, M. W. Germann, N. V. Hud, M. Orozco, *J. Am. Chem. Soc.* **2014**, *136*, 3075–3086; b) W. B. Melchior, P. H. Von Hippel, *Proc. Natl. Acad. Sci. USA* **1973**, *70*, 298–302; c) W. A. Rees, T. D. Yager, J. Korte, P. H. von Hippel, *Biochemistry* **1993**, *32*, 137–144; d) N. V. Hud, A. E. Engelhart in *Nucleic Acid-Metal Ion Interactions* (Eds.: S. Neidle, N. V. Hud), The Royal Society of Chemistry, London, **2009**, pp. 71–113.
[8] a) N. V. Hud, F. Feigon, *Biochemistry* **2002**, *41*, 9900–9910; b) M. Marušič, H. Tateishi-Karimata, N. Sugimoto, J. Plavec, *Biochimie* **2015**, *108*, 169–177; c) N. V. Hud, V. Sklenar, J. Feigon, *J. Mol. Biol.* **1999**, *286*, 651–660; d) M. A. Young, B. Jayaram, D. L. Beveridge, *J. Am. Chem. Soc.* **1997**, *119*, 59–69; e) V. Tereshko, G. Minasov, M. Egli, *J. Am. Chem. Soc.* **1999**, *121*, 3590–3595; f) K. K. Woods, L. McFail-Isom, C. C. Sines, S. B. Howerton, R. K. Stephens, L. D. Williams, *J. Am. Chem. Soc.* **2000**, *122*, 1546–1547; g) G. Minasov, V. Tereshko, M. Egli, *J. Mol. Biol.* **1999**, *291*, 83–99.
[9] X. Q. Shui, C. C. Sines, L. McFail-Isom, D. VanDerveer, L. D. Williams, *Biochemistry* **1998**, *37*, 16877–16887.
[10] I. Gállego, M. A. Grover, N. V. Hud, *Angew. Chem. Int. Ed.* **2015**, *54*, 6765–6769.
[11] F. Wang, X. Liu, I. Willner, *Angew. Chem. Int. Ed.* **2015**, *54*, 1098–1129; *Angew. Chem.* **2015**, *127*, 1112–1144.
[12] S. Chaterji, I. K. Kwon, K. Park, *Prog. Polym. Sci.* **2007**, *32*, 1083–1122.
[13] D. M. John, K. M. Weeks, *Protein Sci.* **2000**, *9*, 1416–1419.
[14] P. Plateau, M. Gueron, *J. Am. Chem. Soc.* **1982**, *104*, 7310–7311.
[15] B. Hess, C. Kutzner, D. van der Spoel, E. Lindahl, *J. Chem. Theory Comput.* **2008**, *4*, 435–447.
[16] A. Pérez, I. Marchan, D. Svozil, J. Sponer, T. E. Cheatham 3rd, C. A. Laughton, M. Orozco, *Biophys. J.* **2007**, *92*, 3817–3829.

Received: April 24, 2015
Revised: June 17, 2015
Published online: July 24, 2015

